CHIME ages of Mg-rich garnet-bearing gneiss clasts from the Jurassic Sawando conglomerate in the northeastern Mino terrane, central Japan

Shiro TANAKA , Kazuhiro SUZUKI and Mamoru ADACHI

Department of Earth and Planetary Sciences, Graduate School of Science,
Nagoya University, Chikusa-ku, Nagoya 464-8602, Japan
Center for Chronological Research, Nagoya University,
Chikusa-ku, Nagoya 464-8602, Japan
The Nagoya University museum, Nagoya University,
Chikusa-ku, Nagoya, 464-8601, Japan

ABSTRACT

CHIME (chemical Th-U-total Pb isochron method) has been applied to determine the ages of two gneiss clasts which are bearing Mg-rich garnet (pyrope content up to 30-40 mol%) from the Jurassic Sawando conglomerate in the northeastern Mino terrane, central Japan. The CHIME monazite ages of gneiss clasts range from 1809 to 1494 Ma with two data concentrations of 1750-1700 Ma and 1650-1600 Ma (sample Sawa-13), and from 1601 to 1040 Ma with a data concentration of 1300-1200 Ma (sample Sawa-43). A detrital zircon in the gneiss clast (Sawa-13) gives the oldest CHIME age of 2064 ±146 Ma. These CHIME age of the gneiss clasts indicate occurrence of middle Precambrian poly-phase meramorphism (between ca. 1800 and 1000 Ma) and igneous activity (ca. 2050 Ma), and suggest that the Mg-rich garnet-bearing gneisses were formed by the middle Precambrian metamorphism.

Detrital garnets, mostly Mg-rich garnet, are commonly observed in the Jurassic sandstone of the Mino terrane. Mg-richgarnet-bearingrockslike the analyzed gneiss clasts are considered as major source rocks of the Jurassic clastsintheMinoterrane. The CHIME ages of the gneiss clasts suggest that a part of the Jurassic terrigenous clastics, for example detrital monazite and Mg-rich garnet in the Mino terrane were derived from the area which is underlain by middle Precambrian metamorphic and igneous rocks.

INTRODUCTION

Provenance analysis on clastic rocks is important for the reconstruction of geological history, since characteristics of clastic rocks have reflected tectonics and geological setting. Recent development of dating method has made spot dating on mineral grain. CHIME (chemical Th-U-total Pb isochron method: e.g. Suzuki et al., 1991; Suzuki and Adachi, 1991a, 1991b; Suzuki et al., 1999) is one of the spot dating method adapted for fine mineral grains including Th, U, and Pb like zircon and monazite. This report focuses on chronological analysis with CHIME for the Mg-rich garnet-bearing gneiss clasts (pyrope content up to 30-40 mol%; Tanaka and Adachi, 1999) from the Jurassic Sawando conglomerate of northeastern Mino terrane, central

Japan, and discuss the relationship between sandstone grains and clasts in the conglomerate.

The Mino terrane which widely occupies central Japan is Jurassic to lower most Cretaceous acrretionary complex, mainly composed of sandstone, shale, chert, limestone and greenstone (e.g. Otsuka, 1988; Wakita, 1988). On the terrigenous detrital grains, Suzukiet al. (1991) and Adachi and Suzuki (1994) have reported a large number of CHIME ages of detrital monazite from Jurassic sandstone. Their data revealed that metamorphic and/or igneous rocks of middle Precambrian to Middle Jurassic age are the major origins of detrital monazites, nevertheless the type of original rocks are still unknown except for some middle Precambrian gneiss (e.g. Shibata and Adachi, 1974; Adachi and Suzuki, 1993).

In the Mino terrane, intraformational conglomerates that contain clasts of granitoid and gneiss are present (e.g. Kanuma and Irie, 1962; Adachi, 1971; Hattori et al., 1985; Otsuka, 1985, 1988; Nakano et al., 1995). Though gneiss clasts are rare in the conglomelates, these are important for the provenance analysis based on petrologic features. The Jurassic sandstones contain abundant clastic plagioclase and Mg-rich garnet derived from metamorphic rocks (Mizutani, 1959; Suzuki, 1977). Mg-rich garnet has been formed under upper amphibolite to granulite facies conditions (e.g. Miyashiro, 1953). Some gneiss clasts from the Jurassic Sawando conglomerate in the northeastern Mino terrane are characterized by containing Mg-rich garnet (Tanaka and Adachi, 1999). To clarify the chronological setting of the Mg-rich garnet-bearing gneiss clasts is also important for recognizing the origin of detrital Mg-rich garnet.

GEOLOGICAL SETTING

The Mino terrane situated in central part of the Japanese Islands is Jurassic to lower most Cretaceous accretionary complex composed mainly of sandstone, shale, chert, limestone and greenstone (e.g. Otsuka, 1988; Wakita, 1988). Microfossil analysis has reconstructed paleo-oceanic plate stratigraphy: Permian greenstone, limestone and chert, Triassic to Jurassic chert and siliceous shale, and Jurassic sandstone and shale (e.g. Otsuka, 1988; Wakita, 1988). The mino terrane is sucdivided into several geological complexes based on lithology, structure and age (e.g. Otsuka, 1988; Wakita, 1988; Nakae, 2000; Yamakita and Otoh, 2000). Figure 1 shows the distribution and subdivision of the northeastern part of the Mino terrane.

In this srudy, specimens are sampled from the Sawando conglomerate (Tanaka et al., 1952) in the Sawando complex (Otsuka, 1988; Fig. 2). The Shirahone complex (Otsuka, 1988) which consists mainly of greenstone and Permian limestone and chert is thrust over the Sawando complex. The Sawando complex consists of the repetition of chert, siliceous shale, shale and alternating beds of sandstone and shale. Otsuka (1985) named this succession as "the chert-clastics sequence" and interpreted that the lithological transition reflects the change of sedimentary environment from pelagic to hemipelagic. Sandstone and shale occupy the majority of the Sawando complex. In the shale-dominant beds, shale is alternated with fine-grained sandstone. In the sandstone-dominant beds, some sandstone is massive and usually has coarse to very coarse grain size with shale patches. Sandstone and shale beds, most commonly distributed,
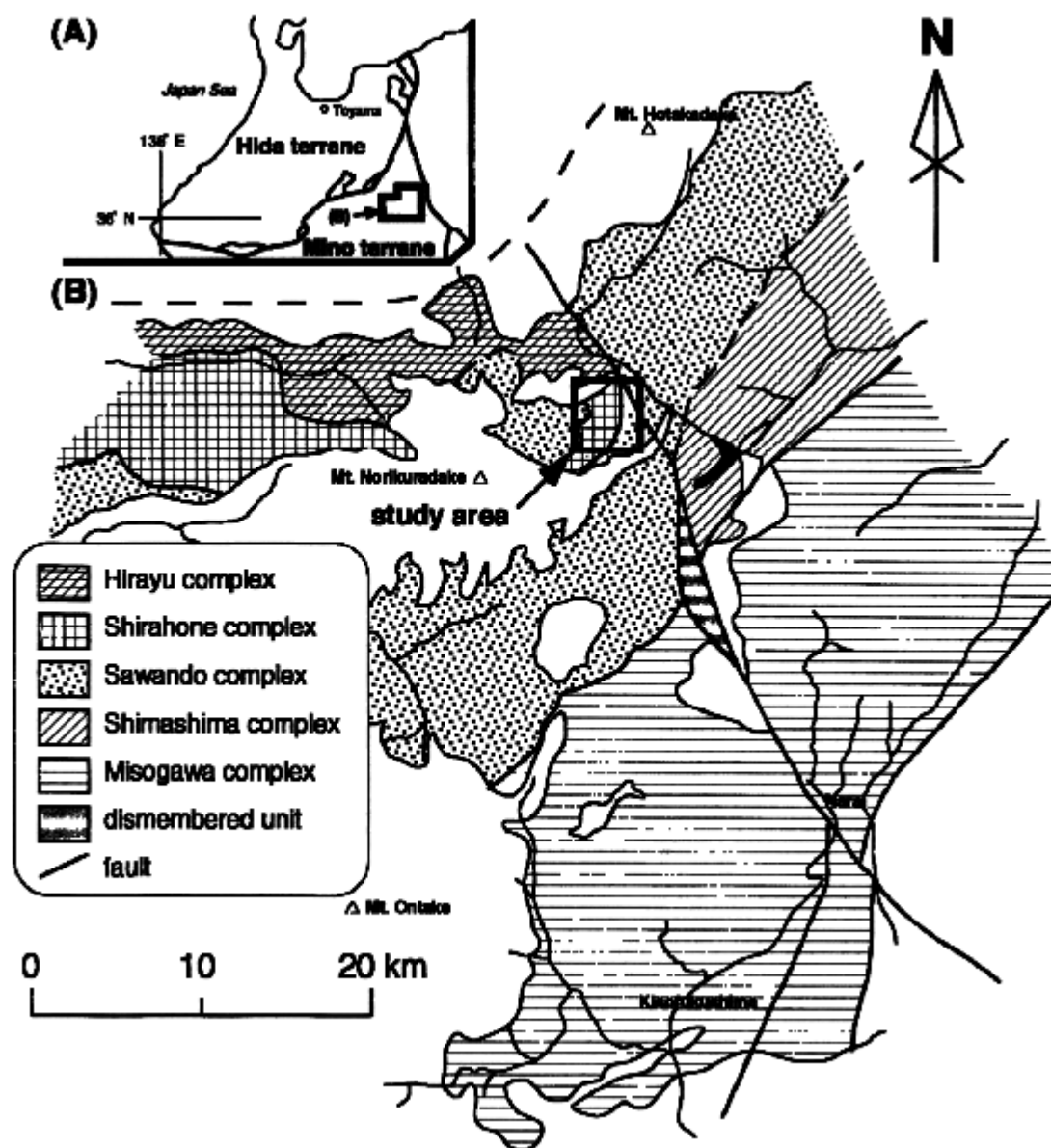
Fig. 1. Index map showing the study area and the distribution of five geological complexes in the northeastern part of the Mino terrane (modified from Otsuka and Watanabe, 1992).

trend northeast and dip northwest. Cross bedding and grading indicate that most of the strata are normal. Sandstone rarely passes into granule conglomerate. Sandstone consists of quartz, potassium feldspar (both orthoclase and microcline), minor plagioclase, and rock fragments of limestone, shale, chert, acidic igneous rock, gneiss and rarely granophyre and sillimanite (fibrolite) gneiss, with heavy minerals such as biotite, muscovite, zircon, agrnet, tourmaline, apatite, rutile and opaque minerals. The Sawando conglomerate is associated with alternating beds of sandstone and shale, and estimated thickness of the conglomerate layer is more than 50 m.

The Sawando conglomerate is poorly sorted, matrix-supported, intraformational and polymict. This conglomerate includes clasts of sandstone and calcareous sandstone
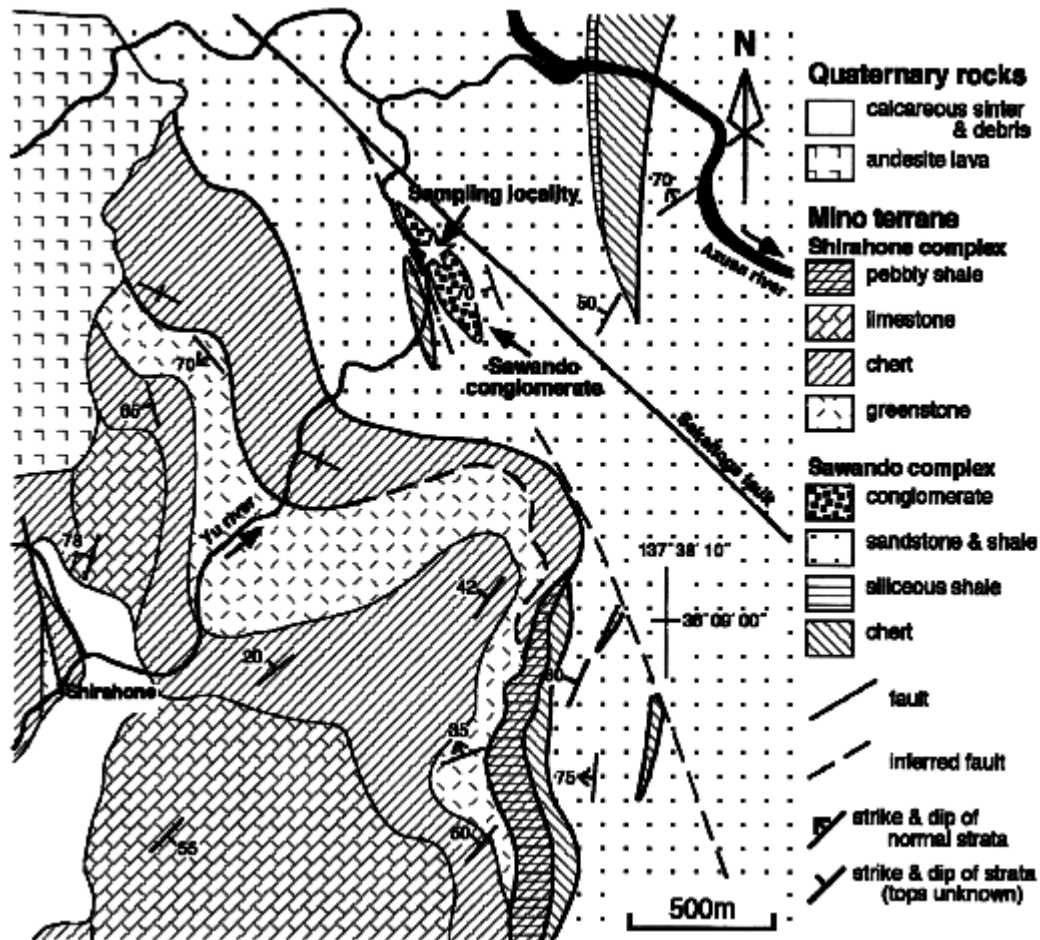
Fig. 2.   Geological map of the study area. Star symbol shows sampling locality.

(23%), shale (25.5%), chert (14%), marl (13%), limestone (2.5%), acidic-intermediate volcanic to hypabyssal rocks (9%), granitoid (2.5%) and metamorphic rocks (0.5%). Clast size is from granule to boulder. Clasts are usually subrounded to well-rouded. Igneous rocks and gneiss clasts are usually rounded to well-rounded shape, bur pebbles of chert, shale and acidic tuff tend to be more angular. Matrix of the conglomerate is usually sandstone but partially muddy sandstone. Imbrication and grading of clasts are not observed. Radiolarian fossils obtained from the Sawando complex (Otsuka, 1985, 1988) provide a late Middle Jurassic age for sedimentation of coarse-grained clastic rocks.

METHOD AND MATERIALS

CHIME age analysis

Monazite and zircon grains in conventional polished thin sections were analyzed on a JEOL JCXA-733 electron-probe microanalyzer. Accelerating voltage, probe current and probe diameter were kept at 15 kV, 0.2 μA and 5 μm, respectively. The ThMα, UMβ, PbMα and YLα lines were measured simultaneously with PET crystals. The
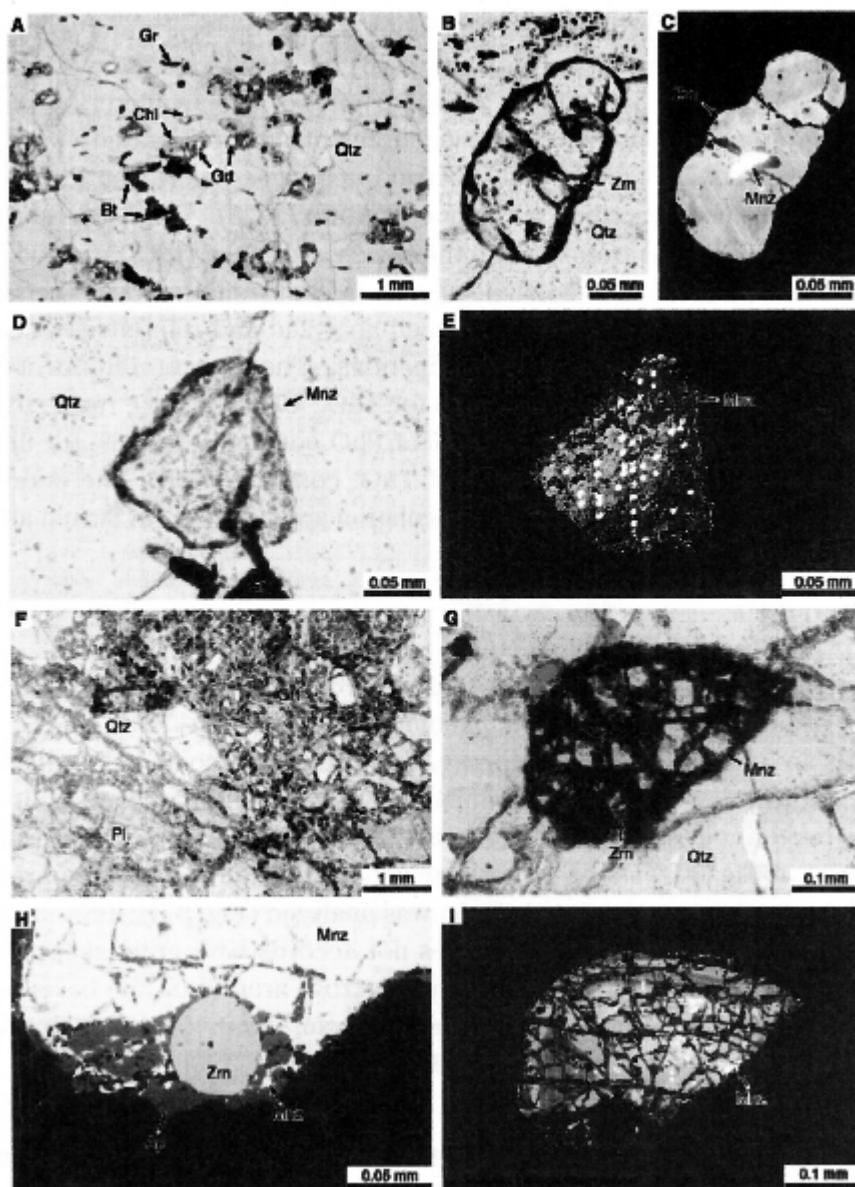
Fig. 3. Photomicrographs and back scattered electron (BSE) images of the gneiss clasts from the Sawando conglomerate in the Mino terrane. A: Texture in the Sawa-13. Garnets, graphite and biotite show weak lateral orientation. One polar. B: Analyzed rounded zircon grain in quartz from the Sawa-13. One polar. C: BSE image of analyzed zircon shows oscillatory zoning and monazite inclusion (white part). Zoning is discordant with grain shape (same grain in Fig. 3-B). D: Analyzed monazite grain in quartz from the Sawa-13. One polar. E: BSE image of analyzed monazite (same grain in Fig. 3-D) from the Sawa-13 shows concentric zoning. Many of light spots are sites for CHIME dating. F: Cracked texture in the Sawa-43. Cracks are filled with calcite (ordinary) and chlorite (in case of garnet). G: Analyzed cracked monazite grain in cracked quartz from the Sawa-43. Crossed polars. H: BSE image of analyzed monazite (same grain in Fig. 3-G) from the Sawa-43. BSE image clearly shows that monazite includes rounded zircon and sececondary apatite. I: BSE image of analyzed monazite (same grain in Figs. 3-G and H) from the Sawa-43. shows concentric zoning which is in accord with grain shape most part. Ap: apatite, Bt: biotite, Chl: chlorite, Gr: graphite, Grt: garnet, Mnz: Monazite, Pl: Plagioclase, Qtz: Quartz, Zrn: Zircon.

standards were euxenite provided by Smellie et al. (1978) for Th and U, and synthesized glass (10.8% PbO; Suzuki and Adachi, 1998) for Pb. X-ray intensities were integrated over 300 seconds by 5-times cyclic stepping of spectrometers on individual peak and background positions. The measurements were repeated twice, and the arithmetic averages were taken. The spectral interference of YLγ on PbMα was corrected with the method described by Åmli and Griffin (1975). The X-ray intensity data were converted into concentrations with the Bence and Albee (1968) method using the analyses of natural zircon and monazite as matrix compositions (Suzuki et al., 1999), since small differences in the matrix between analyzed and reference minerals have little effect on ThO_2, UO_2 and PbO determinations. The detection limits at 1σ confidence level are 0.007, 0.011 and 0.003wt.% for ThO_2, UO_2 and PbO, respectively. The relative errors are about 30% for 0.01 wt.% of PbO concentration, 6% for 0.3 wt.% of UO_2 concentration, and 1% for 10 wt.% of ThO_2 concentration. The details of the analytical procedure and the CHIME age calculation are described in Suzuki and Adachi (1991a) and Suzuki et al. (1991).

Analyzed samples
[Sawa-13]
   This specimen is 6 cm in diameter and well-rounded shape. it is a fine-grained rutile (0.7%)-graphite (1.0%)-garnet (2.3%)-biotite (5.7%)-quartz (82%) gneiss. Secondary minerals are muscovite, chlorite, pyrite, ilmenite and leucoxene. MgO contents of the garnets up to 10 wt.% (about 40 mol% of pyrope). One monazite grain, 150 μm across, has been found and analyzed (Fig. 3-D). Back scattered electron (BSE) image of the monazite (Fig. 3-E) shows concentric zoning. Zircon is usually subrouded to rouded shape, and one subrouded zircon was analyzed (Fig. 3-B). BSE image of this zircon shows oscillatory zoning which does not accords with grain shape (Fig. 3-C). The original rock is assumed to have been quartzose arenite on the basis of texture and mineral composition (Fig. 3-A; Tanaka and Adachi, 1999). Details of this specimen were described in Tanala and Adachi (1999).

[Sawa-43]
   This specimen is about 15 cm in diameter and sub-rounded shape. it is a coarse-grained microcline (very rare)-garnet (0.2%)-biotite (0.2%)-quartz (24.1%)-plagioclase (oligoclase; 74.1%) gneiss. MgO contents of the garnets are about 8 wt.% (about 32 mol% of pyrope). This clast has undergone cataclastic deformation and has had cracks, which are filled with calcite (Figs. 3-F and G). BSE image of the analyzed monazite (Fig. 3-H) shows that monazite includes rounded zircon and has cracks. BSE image of the monazite (Fig. 3-I) shows zoning which partially accords with the grain shape. This specimen was described in Tanaka and Adachi (1999).

RESULTS

   The ThO_2, UO_2 and PbO contents of analyzed monazite and zircon grains, ThO_2* values (ThO_2* values: measured ThO_2 plus ThO_2 equivalent of the measured UO_2) and UO_2* values (UO_2* values: measured UO_2 plus UO_2 equivalent of the measured ThO_2), and apparent ages are listed in Table 1.

Table 1.   Representative analytical data of monazite and zircon in the gneiss clasts from the Sawando comglomerate, in the northeastern part of the Mino terrane.

Sample. Grain No.	ThO$_2$ (wt.%)	UO$_2$ (wt.%)	PbO (wt.%)	Age# (Ma)	ThO$_2$* (wt.%)	Sample. Grain No.	ThO$_2$ (wt.%)	UO$_2$ (wt.%)	PbO (wt.%)	Age# (Ma)	ThO$_2$* (wt.%)
Sawa-13						Mnz01-38	2.62	0.956	0.491	1809	6.18
Mnz01-01	4.92	0.331	0.439	1636	6.13	Mnz01-39	3.05	0.678	0.422	1732	5.56
Mnz01-02	5.14	0.321	0.441	1599	6.31	Mnz01-40	3.28	0.595	0.423	1758	5.49
Mnz01-03	5.33	0.404	0.468	1577	6.80						UO$_2$**
Mnz01-04	5.35	0.386	0.474	1605	6.76	Zrn01-01	0.006	0.014	0.005	2019	0.016
Mnz01-05	4.89	0.476	0.474	1633	6.63	Zrn01-02	0.009	0.021	0.008	2112	0.023
Mnz01-06	5.19	0.413	0.476	1624	6.70	Zrn01-03	0.006	0.052	0.019	2113	0.053
Mnz01-07	5.20	0.388	0.461	1595	6.62	Zrn01-04	0.008	0.011	0.005	2173	0.014
Mnz01-08	5.02	0.354	0.436	1583	6.31	Zrn01-05	0.008	0.037	0.013	2036	0.039
Mnz01-09	5.00	0.353	0.444	1614	6.29	Sawa-43					ThO$_2$**
Mnz01-10	4.83	0.385	0.456	1667	6.25	Mnz01-01	6.49	0.427	0.489	1400	8.02
Mnz01-11	4.68	0.396	0.452	1681	6.14	Mnz01-02	5.99	0.611	0.515	1447	8.18
Mnz01-12	4.68	0.388	0.447	1671	6.11	Mnz01-03	8.41	0.204	0.487	1231	9.13
Mnz01-13	4.73	0.368	0.456	1709	6.09	Mnz01-04	8.36	0.182	0.478	1227	9.00
Mnz01-14	4.52	0.421	0.459	1724	6.07	Mnz01-05	8.43	0.194	0.494	1251	9.11
Mnz01-15	3.35	0.701	0.447	1720	5.93	Mnz01-06	8.30	0.179	0.476	1231	8.93
Mnz01-16	2.83	0.925	0.402	1494	6.17	Mnz01-07	9.20	0.228	0.517	1194	10.00
Mnz01-17	3.41	0.702	0.450	1711	6.00	Mnz01-08	9.30	0.221	0.543	1243	10.08
Mnz01-18	4.06	0.547	0.437	1648	6.06	Mnz01-09	8.30	0.210	0.542	1379	9.05
Mnz01-19	4.58	0.453	0.437	1604	6.23	Mnz01-10	8.96	0.246	0.519	1221	9.83
Mnz01-20	4.37	0.395	0.441	1724	5.83	Mnz01-11	9.89	0.240	0.528	1140	10.72
Mnz01-21	4.44	0.398	0.451	1741	5.91	Mnz01-12	8.69	0.210	0.475	1166	9.42
Mnz01-22	4.18	0.395	0.425	1717	5.64	Mnz01-13	7.32	0.420	0.482	1264	8.81
Mnz01-23	4.30	0.437	0.451	1739	5.92	Mnz01-14	8.39	0.231	0.475	1192	9.20
Mnz01-24	4.80	0.398	0.469	1706	6.27	Mnz01-15	15.53	0.385	0.755	1040	16.86
Mnz01-25	4.36	0.269	0.385	1644	5.35	Mnz01-16	8.00	0.231	0.499	1306	8.81
Mnz01-26	3.68	0.516	0.406	1663	5.58	Mnz01-17	4.78	0.644	0.444	1438	7.09
Mnz01-27	4.32	0.415	0.448	1745	5.86	Mnz01-18	7.52	0.318	0.485	1293	8.64
Mnz01-28	4.35	0.412	0.453	1757	5.88	Mnz01-19	0.012	0.114	0.030	1601	0.429
Mnz01-29	3.98	0.473	0.432	1720	5.73	Mnz01-20	0.019	0.257	0.065	1568	0.954
Mnz01-30	3.94	0.496	0.435	1719	5.77						
Mnz01-31	2.28	0.928	0.445	1770	5.72	MnZ: monazite					
Mnz01-32	3.99	0.469	0.432	1723	5.72	Zrn: zircon					
Mnz01-33	4.27	0.428	0.444	1733	5.85	# : apparent age					
Mnz01-34	2.96	0.744	0.445	1770	5.73	* : sum of the measured ThO$_2$ and ThO$_2$ equivalent					
Mnz01-35	2.46	0.910	0.457	1783	5.84	of the measured UO$_2$					
Mnz01-36	3.05	0.739	0.447	1758	5.79	**: sum of the measured UO$_2$ and UO$_2$ equivalent					
Mnz01-37	3.99	0.426	0.382	1577	5.54	of the measured ThO$_2$					

[Sawa-13]

A total of 5 points on a rounded zircon grain were analyzed. The ThO$_2$ content varies from 0.006 to 0.009 w.%, UO2 from 0.011 to 0.052 wt.%, and PbO from 0.005 to 0.019 wt.%. Apparent ages are from 2019 to 2173 Ma. On the PbO vs. ThO$_2$* diagram, thse data define an isochron of 2064±146 Ma (Fig. 4-C).

A total of 40 points on 1 monazite grain were analyzed. The ThO$_2$ content varies from 2.28 to 5.35 wt.%, UO$_2$ from 0.269 to 0.956 wt.%, and PbO from 0.382 to 0.491 wt.%. Apparent ages of the monazite grains range from 1809 to 1494 Ma, and cluster around 1750-1700 Ma and 1650-1600 Ma (Figs. 4-A and 5-A). In the moanzite grain, distributions of apparent ages are divided into two areas whose boundary is about 1700 Ma (Figs. 5-A and 6). This age distribution is not in accord with concentric zoning pattern shown in BSE image (Figs. 3-E and 6). Its contrast pattern (Fig. 3-E) is in accord well with UO$_2$ and ThO$_2$ contents, and grain shape of monazite (Fig. 6).

[Sawa-43]

The cracked monazite was analyzed at 20 points. The ThO_2 content varies from 0.012 to 15.5 wt.%, UO_2 from 0.114 to 0.644 wt.% and PbO from 0.030 to 0.755 wt.%. Apparent ages are from 1601 to 1040 Ma, and cluster around 1300-1200 Ma (Figs. 4-B and 5-B). Two analyzed points show exceptionally low ThO_2, UO_2 and PbO contents and older apparent ages (1601 and 1568 Ma), while one point shows higher these contents and younger apparent age (1040 Ma).
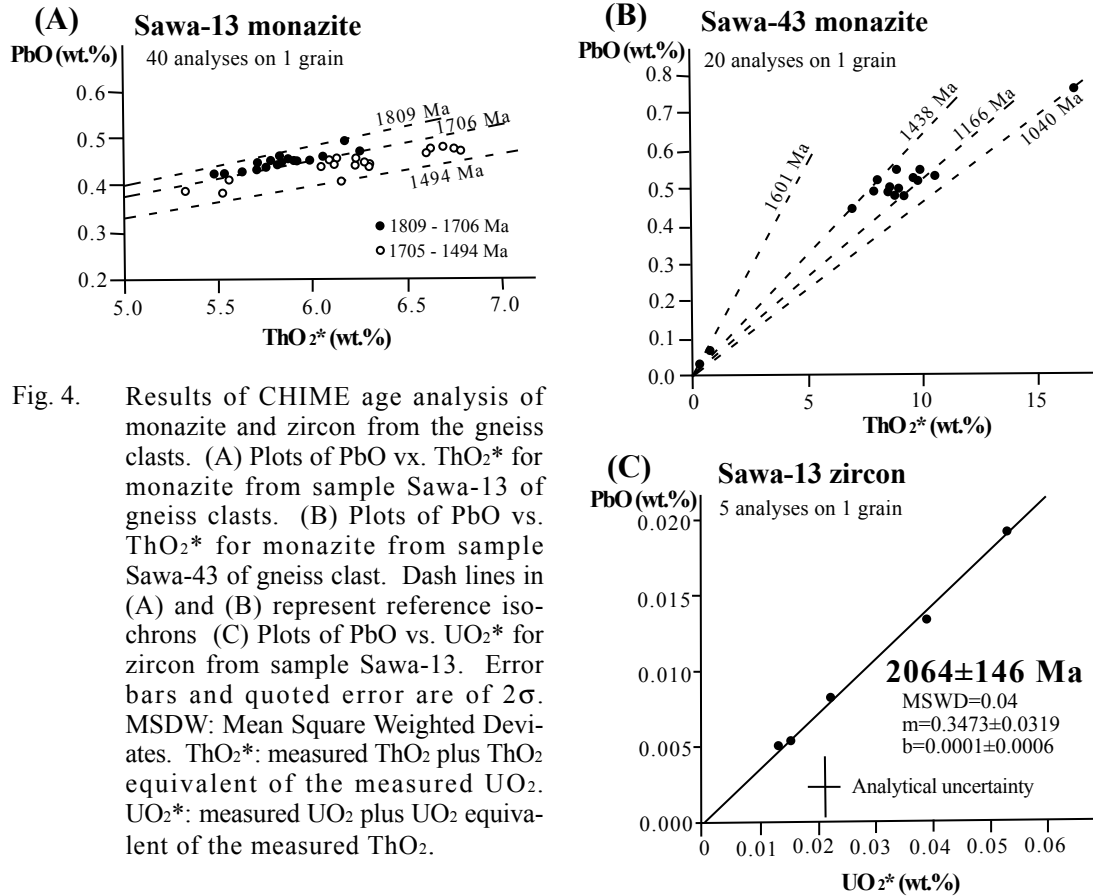
Fig. 4.   Results of CHIME age analysis of monazite and zircon from the gneiss clasts. (A) Plots of PbO vx. ThO_2* for monazite from sample Sawa-13 of gneiss clasts. (B) Plots of PbO vs. ThO_2* for monazite from sample Sawa-43 of gneiss clast. Dash lines in (A) and (B) represent reference isochrons (C) Plots of PbO vs. UO_2* for zircon from sample Sawa-13. Error bars and quoted error are of 2σ. MSDW: Mean Square Weighted Deviates. ThO_2*: measured ThO_2 plus ThO_2 equivalent of the measured UO_2. UO_2*: measured UO_2 plus UO_2 equivalent of the measured ThO_2.
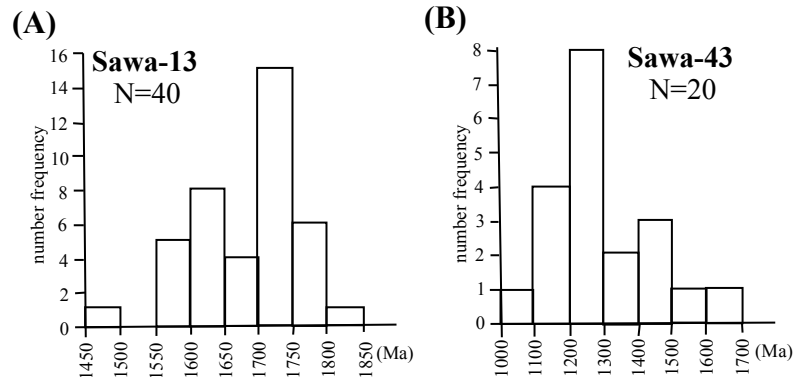
Fig. 5.   Histograms of apparent CHIME ages for monazite from Sawa-13 (A) and Sawa-43 (B). N: number of analysis.
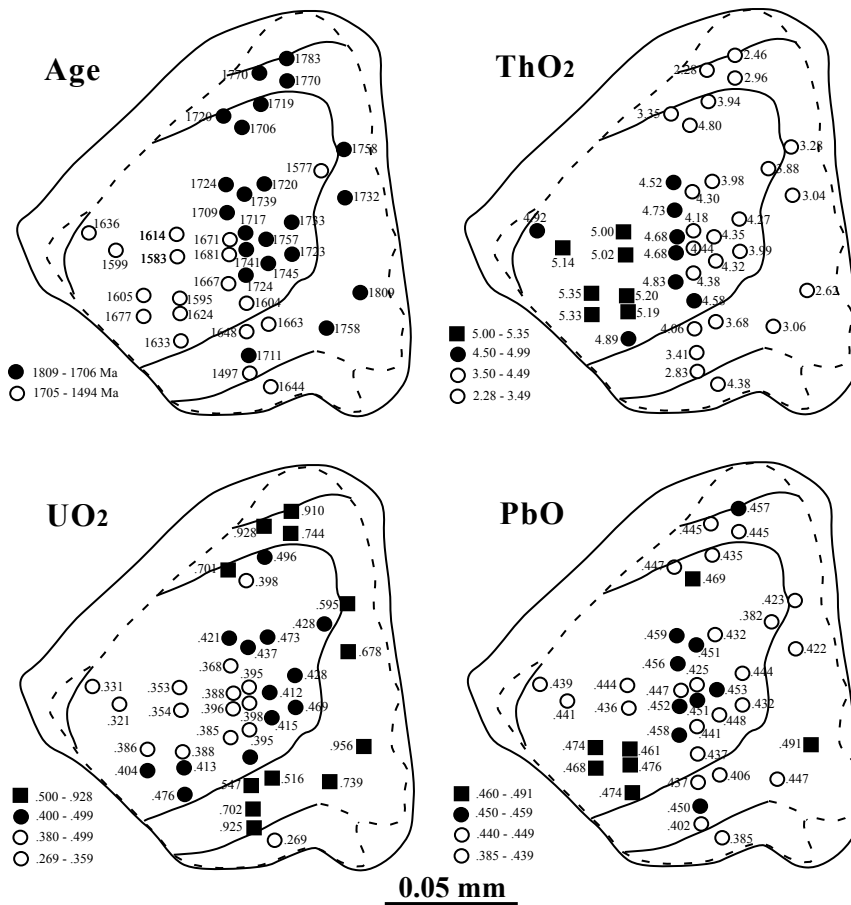
Fig. 6.   Distribution of apparent CHIME ages, and ThO2, UO₂ and PbO contents (wt.%), and concentric zoning (fine solid line) in BSE image of Mnz-01 from Sawa-13. Solid circle, open circle and solid square indicate analyzed spots which correspond to light spots in BSE image of Fig. 3-E. BSE image's contrast is in accord with ThO2 and UO₂ contents. On the other hand, distribution of CHIME ages is discordant with BSE image. Grain shape in BSE image (dash line) is different from the shape observed in microscope (coarse solid line. See Fig. 3-E).

DISCUSSION

CHIME ages of gneiss clasts

The gneiss clasts yield middle Precambrian CHIME monazite ages. Though data points of Sawa-13 and Sawa-43 are not arrayed linearly on the PbO vs. ThO₂* diagrams (Figs. 4-A and B) these ages cluster around 1750-1700 Ma and 1650-1600 Ma, and 1300-1200 Ma, respectively. Overstreet (1967) indicated that monazite in pelitic rock was formed under lower amphibolite facies metamorphism. In addition, lower limit of monazite-forming temperature is estimated about 525±25 °C in pelitic schists in Appalachia (Smith and Barreiro, 1990). Since the gneiss clasts have suffered upper amphibolite facies metamorphism, the analyzed monazites are thought to show ages of metamorphism. It, however, is not clear whether the analyzed monazites are originally detrital or not detrital, because analyzed monazite was only one grain from each clast.

Of the Sawa-13, the analyzed monazite could be considered as either originally detrital (1) or not detrital (2). In the case (1), 1750-1700 Ma is regarded as thermal event before sedimentaiton of quartzose sandstone. 1650-1600 Ma shows metamorphosed age of the gneiss. In the case (2), both 1750-1700 Ma and 1650-1600 Ma are regarded as metamorphosed age of the Sawa-13. Both cases, ca. 1650-1600 Ma shows metamorphosed age of the Sawa-13.

The zircon in the Sawa-13 is thought to be a detrital grain because of its rounded shape. In addition, zoning in BSE image is discordant with grain shape, and shows no distinct overgrowth formed by metamorphism (Fig. 3-C). Oscillatory zoning of zircon shows that this grain was originally formed in igneous rocks, so ca. 2064 Ma indicates the age of igneous activity as forming zircon before sedimentation of quartzose arenite.

Of the Sawa-43, zoning in the BSE image of the monazite seems that this grain is fractured (detrital grain, or fractured and displaced after metamorphisms) or subhedral grain, because lower right part of the grain looks like to be lacked (Figs. 3-G and I). Whereas upper right corner of the grain is angular, so this grain seems not to be detrital. Furthermore, the monazite occurs in single quartz grain; this quartz grain is cracked but all fragments of quartz around the monazite are optionally continuous and are not displaced. Therefore, we regarded the monazite as subhedral grain which was formed during metamorphism, and cluster of apparent ages around 1300-1200 Ma and a minor data concentration around 1400 Ma could be regarded as ages of metamorphisms, The youngest age of 1040 Ma probably indicates the age of thermal event. The oldest stages of 1601 and 1568 Ma may remnant of previous igneous activity or metamorphism, though obtained data of these two points have exceptionally low ThO_2 and PbO contents. Since analyzed points are only at inner part of the zoning, the Sawa-43 may record younger thermal events at rim part. More detailed dating is necessary to be clear the thermal history of the clast. Consequently, the protolith of the Sawa-43 is metamorphosed at middle Precambrian (ca. 1400, 1300-1200 and 1040 Ma), and might be metamorphosed at unidentified younger period.

Relationship between the gneiss clasts and sandstone grains

Suzuki et al. (1991) and Adachi and Suzuki (1994) reported CHIME age of detrital monazite from the Jurassic sandstone in the Mino terrane. According to their reports, apparent ages of detrital monazite grains are especially concentrated between 1740 and 1420 Ma, and between 274 and 161 Ma, and also lie along 1250, 800 and 400 Ma reference isochrons. These spectrum peaks of the detrital monazite age frequency are correlated well with peaks of monazite age frequency from the gneiss clasts (Fig. 5): 1750-1700 Ma, 1650-1600 Ma, 1400 Ma and 1300-1200 Ma. This suggests that 1800-1000 Ma detrital monazites in the sandstones were derived from poly-metamorphosed gneisses. In addition, Tanaka and Adachi (1999) indicated the importance of sample Sawa-13 and Sawa-43 as origin of detrital Mg-rich garnet (pyrope content up to 30-40 mol%) which is usually occurred in the Jurassic sandstone of the Mino terrane (e.g. Suzuki, 1977; Adachi and Kijima, 1983; Tanaka, 2001). The CHIME ages of the gneiss clasts also revealed that detrital Mg-rich garnets in the Jurassic sandstone of the Mino terrane had been derived from the middle Precambrian metamorphic rocks.

Ca. 2064 Ma CHIME zircon age from the Sawa-13 corresponds to 2058±89 Ma

detrital zircon from sandstone in the Mino terrane (Adachi and Suzuki, 1994). Two similar ages were also reported; 2050±50 Ma CHIME zircon age of the quartzo-feldspathic gneiss clast (sample 4-50; Adachi and Suzuki, 1993) and 2050±30 Ma Rb-Sr whole-rock isochron age of gneiss clasts (including sample 4-50; Adachi et al., 1992, recalculated from Shibata and Adachi, 1974) from the Kamiaso conglomerate in the central Mino terrane which is correlated with the Sawanso conglomerate (Adachi, 1976). Ca. 2050 Ma is presumably emplacement time of granitoids, some ot which are undergone ca. 1700 Ma metamorphism (Shibata and Adachi, 1974; Adachi and Suzuki, 1993).

On the other age data from the Jurassic clastic rocks, Suzuki et al. (1991) reported ca. 1740 Ma (core) and 1420 Ma (rim) Ma apparent ages of monazite from the garnet-silliman-ite gneiss clast (sample 4-50) from the Kamiaso conglomerate. This also shows poly-metamorphised gneiss as source rock of the detrital monazites in the Mino terrane. Adachi et al. (1992) reported 1660-959 Ma of K-Ar and 1750-1370 Ma or Rb-Sr mineral ages for biotite, muscovite, plagioclase and K-feldspar for gneiss clasts, some of which form above mentioned ca. 2050 and 1880 Ma whole-rock isochrons. These K-Ar and Rb-Sr mineral ages are probably ages of metamorphism and thermal event, and are roughly corresponded to cluster of monazite ages from gneiss clasts and sandstone.

Consequently, the source rocks of detrital monazite showing middle Precambrian age in the Jurassic sandstone of the Mino terrane are igneous rocks and gneisses which have upper amphibolite facies. According to the present data, each gneiss clast from the Mino terrane records a few middle Precambrian thermal events, nevertheless records no Paleozoic and Mesozoic events. In present, souorce rocks of the detrital monazite younger than 1000 Ma is still not clear, except for ca. 180 Ma granodiorite clast (Tanaka et al., 2000) and Paleozoic detrital moanzite in the orthoquartzite clast (Adachi and Suzuki, 1997) from the jurassic conglomerates.

As for middle Precambrian, preliminary comparison shows that distribution of spectrum peaks of CHIME ages from the sandstone (Suzuki et al., 1991) and gneiss clasts in the Mino terrane are similar to the distribution of radiometric age data for granitoids and metamorphic rocks in the North China region reported by Yang et al (1986), which is one of the candidate for the provenance of hte Jurassic clastics in the Mino terrane.

SUMMARY

(1) The Mg-rich garnet-bearing gneiss clasts were formed by poly-phase middle Precambrian metamorphisms. These gneisses are thought to be source rocks of the detrital Mg-rich garnet in the Jurassic sandstone of the Mino terrane.
(2) Some Precambrian detrital monazites (ca. 1800-1000 Ma) were derived from poly-metamorphosed gneisses and igneous rocks.
(3) Zircon in the gneiss clast indicates ca. 2050 Ma igneous activity. This zircon grain is considered as detrital grain based on morphology and older age than monazite.
(4) The poly-metamorphosed gneiss clasts from the Jurassic conglomerate in the Mino terrane have no record of Paleozoic and Mesozoic thermal events.

ACKNOWLEDGEMENTS

REFERENCES

Adachi, M. (1971) Permian intraformational conglomerate at Kamiaso, Gifu Prefecture, central Japan. *J. Geol. Soc. Japan*, **77**, 471-482.

Adachi, M. (1976) Paleogeographic aspects of the Japanese Paleozoic-Mesozoic geosyncline. *J. Earth Sci. Nagoya Univ.*, **23/24**, 13-55.

Adachi, M. and Kojima, S. (1983) Geology of the Mt. Hikagedaira area, east of Takayama, Gifu Prefecture, central Japan. *J. Earth Sci. Nagoya Univ.*, **31**, 37-67.

Adachi, M., Kijima, S., Wakita, K., Suzuki, K. and Tanaka, T. (1992) Transect of central Japan: from Hida to Shimanto. *29th IGC Field Trip Guide book*, **1**, 143-178.

Adachi, M. and Suzuki, K. (1993) Were Precambrian gneiss clasts in the Kamiaso conglomerate derived from the eastern Korean Peninsula? *Bull. Nagoya Univ. Furukawa Museum*, No. 9, 25-45.*

Adachi, M. and Suzuki, K. (1994) Precambrian detrital monazites and zircons from Jurassic turbidite sandstones in the Nomugi area, Mino terrane. *J. Earth Planet. Sci. Nagoya Univ.*, **41**, 33-43.

Adachi, M. and Suzuki, K. (1997) CHIME monazite ages for orthoquartzite clasts from Mesozoic conglomerates in the Mino and Hida terranes. *Abstr. 1997 Japan Earth Planet. Sci. Jioint Meet.* 587.***

Åmli, R. and Griffin, W.L. (1975) Microprobe analysis of REE minerals using empirical correction factors. *Amer. Mineral.*, **60**, 599-606.

Bence, A.E. and ALbee, A.L. (1968) Empirical correction factors for the electron microanalysis of silicates and ozides. *J. Geol.*, **76**, 382-403.

Hattori, I., Hattori, A. and Ueyama, K. (1985) Kanmuriyama Conglomerates - Mesozoic conglomerates in the northwestern Mino Terrane: a comparative study of the Mesozoic conglomerates in the Mino and the Hida Terranes in Fukui Prefecture, central Japan. *Mem. Fac. Educ. Fukui Univ.*, Ser. 2, **35**, 33-47.*

Kanuma, M. and Irie, K. (1962) On the geology of the Yoro massif, Gifu Prefecture, Japan. *Bull. Tokyo Gakugei Univ.*, **13**, 211-217.*

Miyashiro, A. (1953) Calcium-poor garnet in relation to metamorphism. *Geochim. Cosmochim. Acta*, **4**, 179-208.

Mizutani, S. (1959) Clastic plagioclase in Permian graywacke from the Mugi area, Gifu Prefecture, central Japan. *J. Earth Sci. Nagoya Univ.*, **7**, 108-136.

Nakae, S. (2000) Regional correlation of the Jurassic accretionary complex in the Inner Zone of Southwest Japan. *Mem. Geol. Soc. Japan*, No. 55, 73-98.*

Nakano, S., Otsuka, T., Adachi, M., Harayama, S. and Yoshioka, T. (1995) *Geology of the Norikuradake district*. With Geological Sheet Map at 1: 50,000, Geol. Surv. Japan, 139p.*

Otsuka, T. (1985) Upper Paleozoic and Mesozoic strata in the northeastern part of the Mino Terrane, Nagano Prefecture, central Japan. *J. Geol. Soc. Japan*, **91**, 583-598.*

Otsuka, T. (1988) Paleozoic-Mesozoic sedimentary complex in the eastern Mino Terrane, central Japan and its Jurassic tectonism. *J. Geosci., Osaka City Univ.*, **31**, 63-122.

Otsuka, T. and Watanabe, K. (1992) Illite crystallinity and low-grade metamorphism of pelitic rocks in the Mino Terrane, central Japan. *Mem. Geol. Soc. Japan*, No. 38, 135-145.*

Overstreet, W.C. (1969) The geologic occurrence of monazite. *US Geol. Surv. Prof. Paper*, **530**, 327p.

Shibata, K. and Adachi, M. (1974) Rb-Sr whole-rock ages of Precambrian metamorphic rocks in the Kamiaso conglomerate from central Japan. *Earth Planet. Sci. Lett.*, **21**, 277-287.

Smellie, J.A.T., Cogger, N. and Herrington, J. (1978) Standards for quantitative microprobe determination of uranium and thorium with additional information on the chemical formulae of davidite and euxenite-polycrase. *Chem. Geol.*, **22**, 1-10.

Smith, H.A.. and Barreiro, B. (1990) Monazite U-Pb dating of staurolite grade metamorphism in pelitic schists. *Contrib. Mineral. Petrol.*, **105**, 602-615.

Suzuki, K. (1977) Clastic high-pyrope garnets in Paleozoic sandstone; Kasuga-mura, Ibi-gun, Gifu Prefecture. *Abstr. 84th Annu. Meet. Geol. Soc. Japan*, 51.***

Suzuki, K. and Adachi, M. (1991a) Precambrian provenance and Silurian metamorphism of the Tsubonosawa paragneiss in the SOuth Kitakami terrane, Northeast Japan, revealed by the chemical Th-U-total Pb isochron ages of monazite, zircon and xenotime. *Geochem. J.*, **25**, 357-376.

Suzuki, K. and Adachi, M. (1991b) The chemical Th-U-total Pb isochron ages of zircon and monazite from the Gray Granite of the Hida Terrane, Japan. *J. Earth Sci. Nagoya Univ.*, **38**, 11-37.

Suzuki, K. and Adachi, M. (1998) Denuation history of the high T/P Ryoke metamorphic belt, southwest Japan: constrains from CHIME monazite ages of gneisses and granitoids. *J. Metamorphic Geol.*, **16**, 23-37.

Suzuki, K., Adachi, M., Kato, T. and Yogo, S. (1999) CHIME dating method and its application to the analysis of evolutional history of orogenic belts. *Chikyukagaku (Geochemistry)*, **33**, 1-22.*

Suzuki, K., Adachi, M. and Tanaka, T. (1991) Middle Precambrian provenance of Jurassic sandstone in the Mino Terrane, central Japan: Th-U-total Pb evidence from an electron microprobe monazite study. *Sediment. Geol.*, **75**, 141-147.

Tanaka, T., Kobayashi, K. and Kamei, T. (1952) Stratigraphic setting of Sawando conglomerate. *Sci. Repts., Fac. Education, Shinshu Univ.*, **2**, 108-116.**

Tanaka, S. (2001) Composition of sandstones in the Mino Terrane - change in detrital garnet chemistry-. *Abstr. 108th Annu. Meet. Geol. Soc. Japan*, 241.***

Tanaka, S. and Adachi, M. (1999) Occurrence of gneiss clasts with Mg-rich garnets from the Sawando conglomerate in the northeastern Mino terrane: source of detrital Mg-rich garnets in the Jurassic sandstone of the Mino terrane. *J. Geol. Soc. Japan*, **105**, 193-199.*

Tanaka, S., Suzuki, K. and Adachi, M. (2000) Preliminary report on ca. 178 Ma granitic rock clast from the Jurassic conglomerate in the Tsukiyozawa area, northeastern Mino terrane, central Japan. *Bull. Nagoya Univ. Museum*, No.16, 66-41.*

Wakita, K. (1988) Origin of chaotically mixed rock bodies in the Early Jurassic to Early Cretaceous sedimentary complex of the Mino terrane, central Japan. *Bull. Geol. Surv. Japan*, **39**, 675-757.

Yamakita, S. and Otoh, S. (2000) Tectonostratigraphic division of accretionalry-sedimentary complex of the Tamba-Mino-Ashio Belt and comparison with the Northern and Southern Chichibu Belts. *Struct. Geol.*, No. 44, 5-32.*

Yang, Z., Cheng, Y. and Wang, H. (1986) *The geology of China.* Clarendon Press, Oxford, 303p.

*: In Japanese with English abstract
**: In Japanese with German abstract
***: In Japanese